A Note on Fatigue Crack Growth Predictions Based on Damage Accumulation Ahead of the Crack Tip

J.T.P. Castro[1], M.A. Meggiolaro, A.C.O. Miranda
Mechanical Engineering Department, Pontifical Catholic University of Rio de Janeiro, Brazil
[1]Corresponding Author: jtcastro@mec.puc-rio.br

Abstract

Models are proposed to predict the fatigue crack growth (FCG) process using crack initiation properties and critical damage concepts. The crack is modelled as a sharp notch with a very small but finite tip radius to remove its singularity, using a strain concentration rule. In this way, the damage caused by each load cycle and the effects of residual stresses can be calculated at each element ahead of the crack tip using the correct hysteresis loops caused by the loading, without the need for adjustable parameters. A quite good agreement between the εN-based crack growth predictions and experiments is obtained both for constant and for variable amplitude load histories.

Introduction

Since the pioneer work of Majumdar and Morrow in 1974 [1], several models have been proposed to correlate the oligocyclic fatigue crack initiation process, controlled by the strain range $\Delta\varepsilon$, with fatigue crack propagation rates, controlled by the stress intensity range $\Delta\mathbf{K}$. Some of this so-called critical damage models consider the width of the volume element in the crack propagation direction as being the distance that the fatigue crack propagates on each cycle **da**. Others consider the fatigue crack propagation rate as being the element width divided by the number of cycles that the crack would need to cross it. However, most models do not properly deal with the supposed stress field singularity at the crack tip, which implies that all damage would be caused by this very last event. Recently, an improved model that deals with the actual elastic-plastic stresses at the crack tip has been proposed [2], using εN parameters and expressions of the HRR type to represent the elastic-plastic strain range inside the plastic zone ahead of the crack tip, which is modeled as a sharp notch with a very small but finite tip radius to remove the singularity issues. The origin of the HRR field is shifted from the crack tip to a point inside the crack, located by matching the HRR strain at the blunt crack tip with the strain predicted at that point by a strain concentration rule.

The models consider that the damage zone ahead of the crack tip is composed by a sequence of very small volume elements, each one under a different strain range, which are being broken sequentially as the crack propagates. Each of these volume elements will be submitted to elastic-plastic hysteresis loops of increasing amplitude as the crack tip approaches it. Any given volume element suffers damage in each load cycle, caused by the amplitude of the loop acting in that cycle, which in turn depends on the distance r_i between the i-th volume element and the fatigue crack tip. Fracturing of the volume element at the crack tip (which causes fatigue crack growth) occurs when its accumulated damage reaches a critical value, due to the sum of the damage suffered in each cycle, quantified by a damage accumulation rule, see Fig. 1.
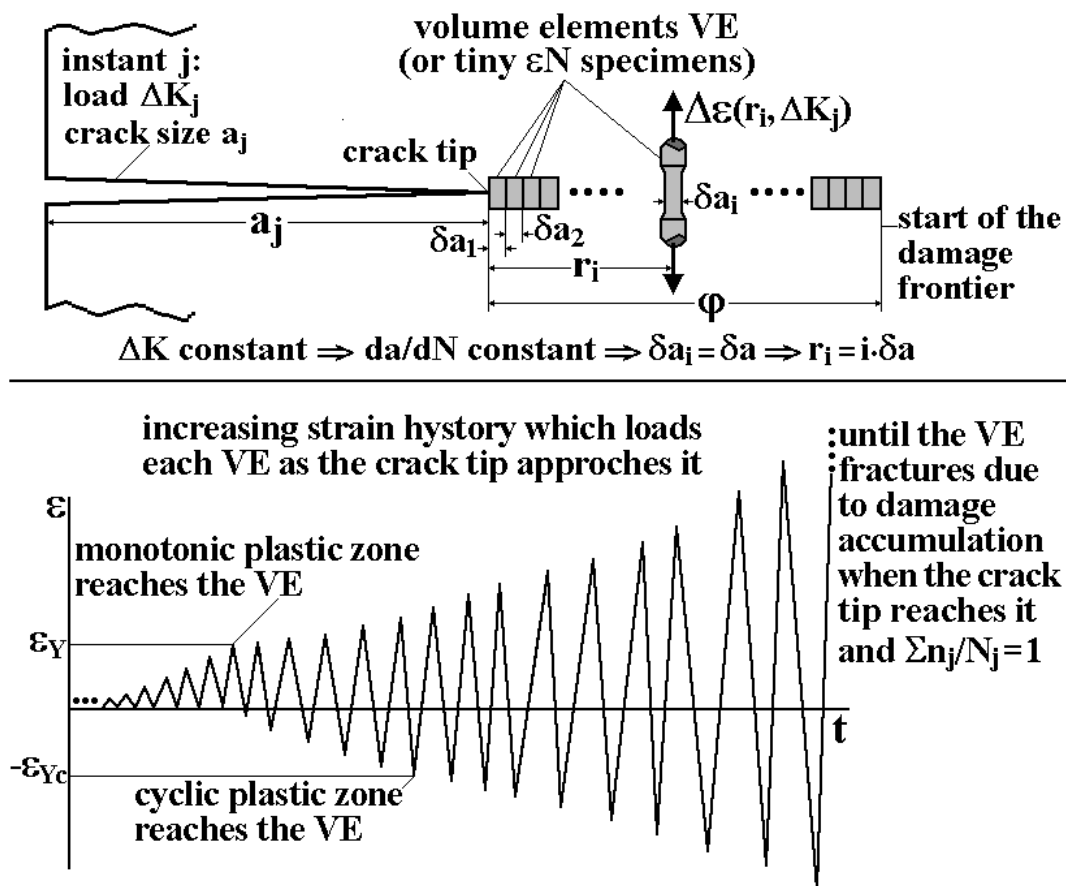
Fig.1: Schematics of the FCG assumed to be caused by the sequential fracture of volume elements (or tiny εN specimens) at every load cycle, loaded by an increasing strain history as the crack tip approaches them.

The idea that FCG is caused by the sequential failure of volume elements ahead of the crack tip can be extended to deal with the variable amplitude loading case. However, there are many mechanisms that can retard or accelerate the growth of a fatigue crack after significant load amplitude

variations [3-6]. Moreover, these mechanisms generally can act simultaneously, with their relative importance in any problem depending on several factors such as crack and piece sizes, dominant stress state at the crack tip, microstructure of the material, mean load, and environment. These load interaction mechanisms can act **behind**, **at** or **ahead** of the crack tip, and among them:

- crack closure (**behind** the crack tip), which can be caused by plasticity, oxidation or roughness of the crack faces, or even by strain induced phase transformation, e.g.;
- crack tip blunting, kinking or bifurcation (**at** or close to the crack tip); and
- residual stress and strain fields (**ahead** of the crack tip).

Most models of load sequence effects in fatigue crack growth (FCG) are still based on Elber's plasticity-induced crack closure, despite some important limitations. However, there are several important problems that cannot be explained by the effective stress intensity range ΔK_{eff} concept. For example, a strong objection against crack closure is based on convincing experimental evidence such as fatigue crack growth threshold values ΔK_{th} that are higher in vacuum than in air [7]. Another very important problem that cannot be explained by the Elber mechanism is the crack delays or arrests after overloads under high $R = K_{min}/K_{max}$ ratios, when the minimum value K_{min} of the applied stress-intensity range $\Delta K = K_{max} - K_{min}$ always remains *above* K_{op}, the (measured) load that opens the fatigue crack [8]. In this case there is no closure nor before nor after the overloads.

The Non-Singular Damage Model

The damage *ahead* of a fatigue crack tip can be estimated using simple but sound hypotheses and standard fatigue calculations, supposing that fatigue cracks grow by sequentially breaking small volume elements (VE) ahead of their tips, which fracture when the crack tip reaches them because they accumulated all the damage the material can support. In this way, εN procedures can be combined with fracture mechanics concepts to *predict* FCG, using the cyclic properties of the material and the strain distribution ahead of the crack tip. These models can consider the VE width in the FCG direction as being the distance that the crack grows on each cycle, or the FCG rate as being the VE width divided by the number of cycles that the crack would need to cross it.

Critical damage models are not new [1, 9-10], but still need improvements. Most models assume singular stress and strain fields ahead of the crack tip (concentrating in this way all the damage next to the tip), and thus need some adjustable constant to fit the FCG **da/dN** data, irreversibly compromising their *prediction* potential in this way. However, the supposed singularity at the crack tip is a characteristic of the mathematical models that postulate a zero radius tip, not of the real cracks, which have a blunt tip when loaded. In other words, real cracks must have finite strains at their tip under load, or else they would be unstable. To avoid this problem, the actual finite strain range at the crack tip $\Delta\varepsilon_{tip}$ can be estimated using the stress concentration factor K_t for the blunt crack [11] and a strain concentration rule. The strain range field ahead of the crack tip can then be upper-bounded by $\Delta\varepsilon_{tip}$ (e.g., by assuming $\Delta\varepsilon_{tip}$ constant where the singular solution would predict strains greater than $\Delta\varepsilon_{tip}$, or by translating the singular strain field, as discussed later).

Some models suppose that all fatigue damage occurs inside this region next to the tip, and use the number of cycles N^* associated with $\Delta\varepsilon_{tip}$ (which can be obtained from Coffin-Manson's rule, e.g.) to calculate the FCG rate can as the length of this region divided by N^*. But such models have two shortcomings. First, neglecting the fatigue damage elsewhere concentrates it in the very last N^* cycles, a non-conservative hypothesis. Second, assuming intermittent and not a cycle-by-cycle fatigue-induced increments in the crack length, although valid in some cases of crazing in polymers, is certainly not true for most metallic structures, as evidenced by their striated cracks surfaces.

To avoid these limitations, the model used here uses Schwalbe's modification [9] of the HRR field to represent the strain range distribution ahead of the crack tip, and removes the crack tip singularity by shifting the origin of the strain field from the crack tip to a point inside the crack, located by matching the tip strain with $\Delta\varepsilon_{tip}$ predicted by a strain concentration rule, such as Neuber [12], Molsky and Glinka [13], or the linear rule [14]. This approach recognizes that the strain range $\Delta\varepsilon(\mathbf{r}, \Delta\mathbf{K})$ in all unbroken VE increases and causes damage in each load cycle as the crack tip approaches them, see Fig. 1. Therefore, the VE closest to the tip breaks due to the sum of the damage induced by all previous load cycles (which under constant amplitude load increases as the distance

of the VE to the crack tip decreases while the crack grows), and not only by the damage induced in the very last load cycle. In this way, the fatigue crack growth rate under constant ΔK can be modeled by the sequential failure of identical VE ahead of the crack tip.

This model is then extended to deal with the variable amplitude loading case, which has idiosyncrasies that must be treated appropriately. First, the VE that breaks in any given cycle has variable width, which should be calculated by locating the point ahead of the crack tip where the accumulated damage reaches a specified value (e.g. 1.0 when using Miner's rule). Load sequence effects, such as overload-induced crack growth retardation, are associated with mean load effects caused by elastic-plastic hysteresis loop shifts, and can be calculated using the powerful numerical tools available in the **ViDa** software [15]. Moreover, this model can recognize an opening load, and thus can separate the cyclic damage from the closure contributions to the crack growth process.

Constant Amplitude Loading

In every load cycle, each VE ahead of the crack tip suffers strain loops of increasing range as the tip approaches it, and a damage increment that depends on the strain range in that cycle, thus on $\mathbf{r_i}$, the distance from the i-th VE to the tip and on the load ΔK_j at that event. The fracture of the VE at the crack tip occurs because it accumulated its critical damage, e.g. by Miner when $\Sigma n_j/N_j = 1$, where $\mathbf{n_j}$ is the number of cycles of the **j**-th load event and $\mathbf{N_j}$ is the number of cycles that the piece would last if loaded solely by that event. If under constant ΔK (or ΔK_{eff}) the fatigue crack advances a fixed distance δa in every load cycle, and if, for simplicity, the damage outside the cyclic plastic zone $\mathbf{zp_c}$ is neglected, there are thus $\mathbf{zp_c/\delta a}$ VE ahead of the crack tip at any instant. Since the plastic zone advances with the crack, each new load cycle breaks the VE adjacent to the crack tip, induces an increased strain range in all other unbroken VE, and adds a new element to the damage zone, thus $\mathbf{n_j = 1}$. Moreover, since the VE are considered as small εN specimens, they break when:

$$\sum_{i=0}^{zp_c/\delta a} \frac{1}{N(zp_c - i \cdot \delta a)} = \sum_{r_i=0}^{zp_c} \frac{1}{N(r_i)} = 1 \qquad (1)$$

where $N(r_i) = N(zp_c - i \cdot \delta a)$, the fatigue life corresponding to the plastic strain range $\Delta\varepsilon_p(r_i)$ acting at a distance r_i from the crack tip, can be calculated using the plastic part of Coffin-Manson's rule:

$$N(r_i) = \frac{1}{2}\left(\frac{\Delta\varepsilon_p(r_i)}{2\varepsilon_c}\right)^{1/c} \tag{2}$$

$\Delta\varepsilon_p(r_i)$ in its turn can be described by Schwalbe's [9] modification of the HRR field:

$$\Delta\varepsilon_p(r_i) = \frac{2S_{Yc}}{E} \cdot \left(\frac{zp_c}{r_i}\right)^{\frac{1}{1+h_c}} \tag{3}$$

where S_{Yc} is the cyclic yield strength, h_c the Ramberg-Osgood cyclic hardening exponent, and zp_c is the cyclic plastic zone size in plane strain, which can be estimated, by (ν is Poisson's coefficient):

$$zp_c = \frac{(1-2\nu)^2}{4\pi \cdot (1+h_c)} \cdot \left(\frac{\Delta K}{S_{Yc}}\right)^2 \Rightarrow N(r_i) = \frac{1}{2}\left[\frac{S_{Yc}}{E\varepsilon_c} \cdot \left(\frac{zp_c}{r_i}\right)^{\frac{1}{1+h_c}}\right]^{1/c} \tag{4}$$

The HRR field describes the plastic strains ahead of an idealized crack tip, thus it is singular at $r = 0$. But an infinite strain is physically impossible (which does not mean that singular models are useless, but only that the damage close to the crack tip is not predictable by them). To eliminate this unrealistic strain singularity, the origin of the HRR coordinate system is shifted into the crack by a small distance X, copying Creager and Paris idea [11]. Approximating the VE width δa by a differential da at a distance dr ahead of the crack tip and the Miner's summation by an integral, which is easier to deal with [2]:

$$\Delta\varepsilon_p(r+X) = \frac{2S_{Yc}}{E} \cdot \left(\frac{zp_c}{r+X}\right)^{\frac{1}{1+h_c}} \tag{5}$$

$$\frac{da}{dN} = \int_0^{zp_c} \frac{dr}{N(r+X)} \tag{6}$$

To determine X and $N(r + X)$ two paths can be followed. The first uses Creager and Paris' $X = \rho/2$, ρ being the actual crack tip radius, estimated by $\rho = CTOD/2$, thus

$$X = \frac{\rho}{2} = \frac{CTOD}{4} = \frac{K_{max}^2 \cdot (1-2\nu)}{\pi \cdot E \cdot S_{Yc}} \cdot \sqrt{\frac{1}{2(1+h_c)}} \tag{7}$$

6

The second path is more reasonable. Instead of arbitrating the strain field origin offset, it determines $\mathbf{X}$ by first calculating the crack (linear elastic) stress concentration factor $\mathbf{K_t}$ [11]:

$$K_t = 2\Delta K \big/ (\Delta\sigma_n \cdot \sqrt{\pi\rho}) \tag{8}$$

For any given $\Delta\mathbf{K}$ and $\mathbf{R}$ it is possible to calculate ρ and $\mathbf{K_t}$ from (7) and (8), and then the strain range $\Delta\varepsilon_{tip}$ at the crack tip using a strain concentration rule. Assuming that the material stress-strain behavior is parabolic with cyclic strain hardening coefficient $\mathbf{H_c}$ and exponent $\mathbf{h_c}$, with a negligible elastic range, the Linear, Neuber and Molsky and Glinka concentration rules give, respectively:

$$\Delta\varepsilon_{tip} = \frac{K_t \cdot \Delta\sigma_n}{E} = \frac{2\Delta K}{E\sqrt{\pi \cdot CTOD/2}} \tag{9}$$

$$\begin{cases} \Delta\sigma_{tip} \cdot \Delta\varepsilon_{tip} = \cdot \dfrac{(K_t \Delta\sigma_n)^2}{E} = \dfrac{8\Delta K^2}{E \cdot \pi \cdot CTOD} \\[2mm] \Delta\varepsilon_{tip} = 2\left(\dfrac{\Delta\sigma_{tip}}{2H_c}\right)^{1/h_c} \end{cases} \tag{10}$$

$$\begin{cases} \dfrac{2\Delta K^2}{E \cdot \pi \cdot CTOD} = \dfrac{\Delta\sigma_{tip}^2}{4E} + \dfrac{\Delta\sigma_{tip}}{1+h_c} \cdot \left(\dfrac{\Delta\sigma_{tip}}{2H_c}\right)^{1/h_c} \\[2mm] \Delta\varepsilon_{tip} = 2\left(\dfrac{\Delta\sigma_{tip}}{2H_c}\right)^{1/h_c} \end{cases} \tag{11}$$

After calculating $\Delta\varepsilon_{tip}$ at the crack tip using one of these rules, the shift $\mathbf{X}$ of the HRR origin is obtained by:

$$\Delta\varepsilon_{tip} = \frac{2S_{Yc}}{E} \cdot \left(\frac{zp_c}{X}\right)^{\frac{1}{1+h_c}} \Rightarrow X = zp_c \cdot \left(\frac{2S_{Yc}}{E\Delta\varepsilon_{tip}}\right)^{1+h_c} \tag{12}$$

The strain distribution at a distance $\mathbf{r}$ ahead of the crack tip, $\Delta\varepsilon_p(\mathbf{r} + \mathbf{X})$, without the singularity problem at the crack tip, can now be readily obtained by:

$$\frac{da}{dN} = \int_0^{zp_c} 2 \cdot \left(\frac{2\varepsilon_c}{\Delta\varepsilon_p(r+X)}\right)^{1/c} dr \tag{13}$$

This prediction was experimentally verified in SAE1020 and API 5L X-60 steels and in a 7075 T6 Al alloy, using (13) to obtain the constant of a McEvily-type $\mathbf{da/dN}$ equation, which describes the $\mathbf{da/dN} \times \Delta\mathbf{K}$ curves using only one adjustable parameter:

$$\frac{\mathbf{da}}{\mathbf{dN}} = A\left[\Delta K - \Delta K_{th}(R)\right]^2 \left(\frac{K_c}{K_c - [\Delta K/(1-R)]}\right) \tag{14}$$

where $\mathbf{K_c}$ and $\mathbf{\Delta K_{th}(R)}$ are the material fracture toughness and crack propagation threshold at the load ratio $\mathbf{R}$. To guarantee the consistence of this experimental verification, $\mathbf{K_c}$, $\mathbf{\Delta K_{th}(R)}$, the $\mathbf{\varepsilon N}$ and the $\mathbf{da/dN}$ data were all obtained by testing proper specimens manufactured from the same stock of the 3 materials, following ASTM standards. The API 5L X-60 $\mathbf{da/dN \times \Delta K}$ experimental curves is compared with this simple model predictions in Fig. 2 (see [2] for the other materials, all of which followed a similar behavior). Both the shape and the magnitude of the data are quite reasonably reproduced by this critical damage model, with the Linear rule generating better *predictions* probably because the tests were made under predominantly plane-ε conditions. Moreover, since this model does *not* use any adjustable constant, this performance is certainly no coincidence.
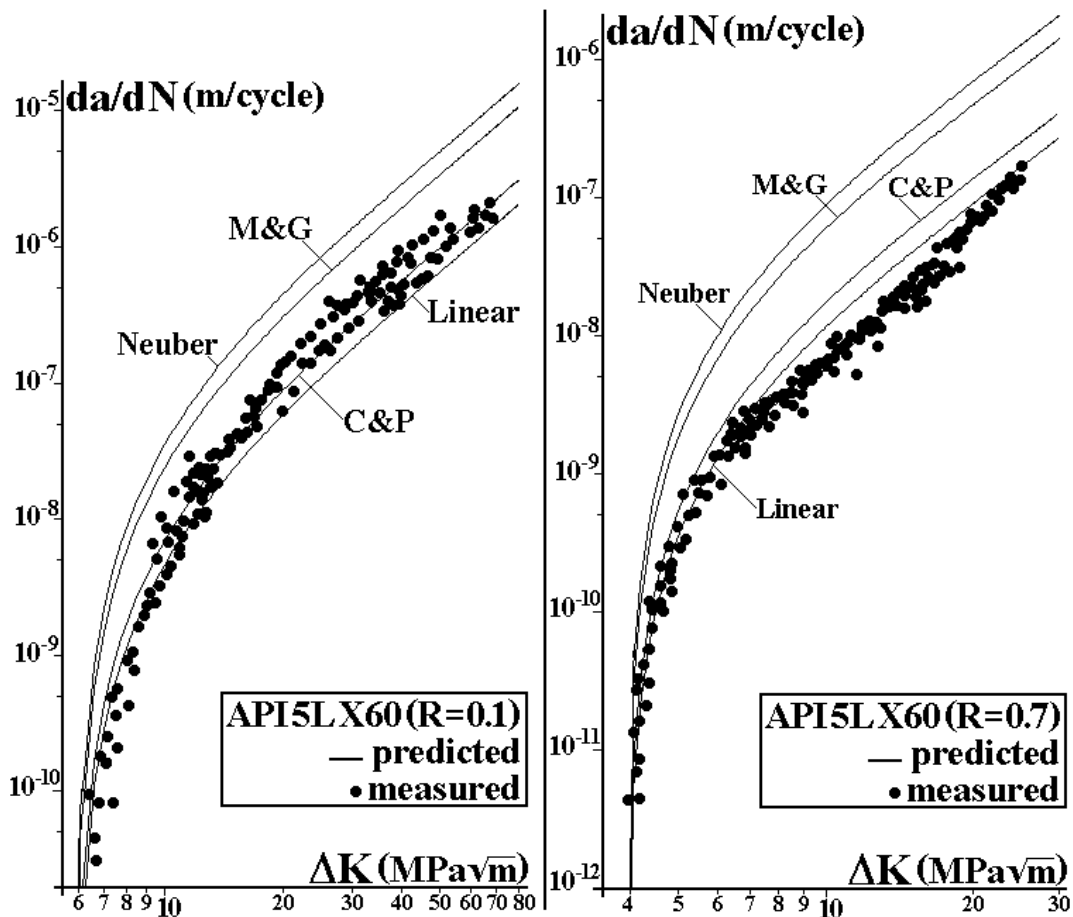
Fig.2: $\mathbf{da/dN \times \Delta K}$ behavior measured and ***predicted*** by the various strain concentration rules used in the critical damage model, for API-5L-X60 pipeline steel at $\mathbf{R = 0.1}$ and $\mathbf{R = 0.7}$.

Despite this encouraging performance, some remarks are still required. First, the damage beyond $\mathbf{zp_c}$ was neglected to simplify the numerical calculations, but as it accumulates at all points

ahead of the crack tip, it is wiser to choose the damage origin by numerically testing its influence on **da/dN**, or better by comparing the predictions with FCG tests, as done later on. Second, FE calculations [16] indicate that there is a region adjacent to the blunt crack tip with a strain gradient much lower than predicted by the HRR field. These problems can be avoided by shifting the origin *away* from the tip by $\mathbf{x_2}$ and assuming the crack-tip strain range $\Delta\varepsilon_{\mathbf{tip}}$ constant over the region I of length $\mathbf{x_1 + x_2}$ shown in Fig. 3, where $\mathbf{x_1}$ can be obtained equating $\Delta\varepsilon_{\mathbf{tip}}$ and the HRR-calculated strain range, and the crack-tip stress range $\Delta\sigma_{\mathbf{tip}}$ from:

$$\Delta\sigma_{\mathbf{tip}} = \Delta\sigma(\mathbf{r} = \mathbf{x_1}) = 2S_{\mathbf{Yc}} \cdot \left(\frac{\mathbf{zp_c}}{\mathbf{x_1}}\right)^{\frac{\mathbf{h_c}}{1+\mathbf{h_c}}} = 2S_{\mathbf{Yc}} \cdot \left(\frac{E \cdot \Delta\varepsilon_{\mathbf{tip}}}{2S_{\mathbf{Yc}}}\right)^{\mathbf{h_c}} \tag{15}$$

Then, following Irwin's classical idea, the value of the shift $\mathbf{x_2}$ is obtained by integrating the stress field $\sigma(\mathbf{r})$, enforcing equilibrium of the applied force:

$$\int_0^\infty \Delta\sigma(\mathbf{r})d\mathbf{r} = \int_0^{\mathbf{x_1+x_2}} \Delta\sigma_{\mathbf{tip}}d\mathbf{r} + \int_{\mathbf{x_1}}^\infty \Delta\sigma(\mathbf{r})d\mathbf{r} \Rightarrow \int_0^{\mathbf{x_1}} \Delta\sigma(\mathbf{r})d\mathbf{r} = \int_0^{\mathbf{x_1+x_2}} \Delta\sigma_{\mathbf{tip}}d\mathbf{r} \tag{16}$$

Since $\mathbf{x_1} < \mathbf{zp_c}$, $\Delta\sigma(\mathbf{r})$ in the above integral can still be described by the HRR solution, resulting in

$$\int_0^{\mathbf{x_1}} 2S_{\mathbf{Yc}} \cdot \left(\frac{\mathbf{zp_c}}{\mathbf{r}}\right)^{\frac{\mathbf{h_c}}{1+\mathbf{h_c}}} d\mathbf{r} = \Delta\sigma_{\mathbf{tip}} \cdot \mathbf{x_1} \cdot (1+\mathbf{h_c}) = \Delta\sigma_{\mathbf{tip}} \cdot (\mathbf{x_1} + \mathbf{x_2}) \Rightarrow \mathbf{x_2} = \mathbf{x_1} \cdot \mathbf{h_c} \tag{17}$$

These simple tricks generate a more reasonable strain distribution model (Fig. 3):

$$\Delta\varepsilon(\mathbf{r}) = \Delta\varepsilon_{\mathbf{tip}} \, , \, 0 \leq \mathbf{r} \leq \mathbf{x_1} + \mathbf{x_2} \text{ (region I)} \tag{18}$$
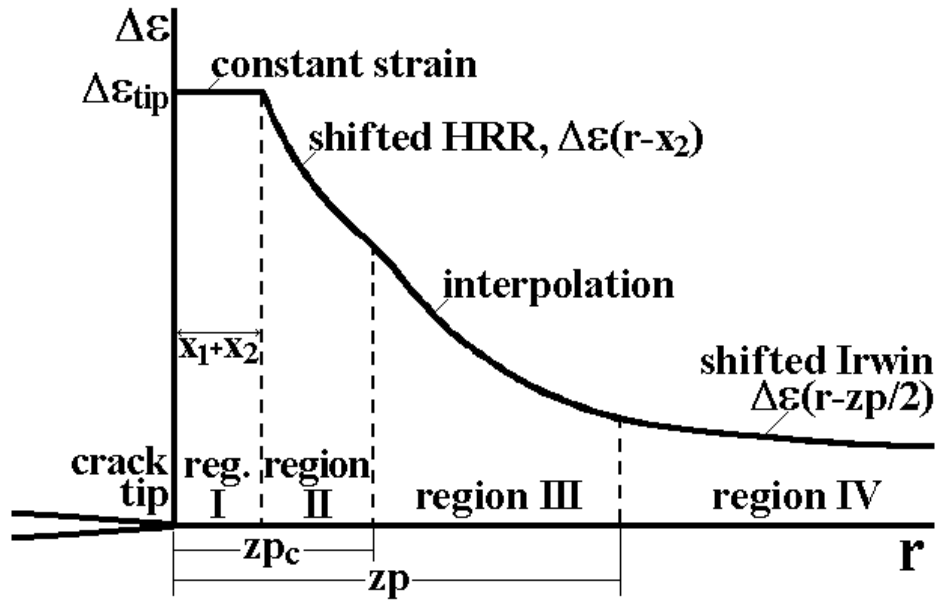
$$\Delta\varepsilon(\mathbf{r}) = \frac{2S_{\mathbf{Yc}}}{E} \cdot \left(\frac{\mathbf{zp_c}}{\mathbf{r} - \mathbf{x_2}}\right)^{\frac{1}{1+\mathbf{h_c}}} , \, \mathbf{x_1} + \mathbf{x_2} < \mathbf{r} \leq \mathbf{zp_c} + \mathbf{x_2} \text{ (region II, shifted HRR)} \tag{19}$$

$$\Delta\varepsilon(\mathbf{r}) \cong \frac{2S_{\mathbf{Yc}}}{E} \cdot \sqrt{\frac{\mathbf{zp_c} + \mathbf{x_2}}{\mathbf{r}}} \cdot (1 + \nu \frac{\mathbf{r} - \mathbf{zp_c}}{\mathbf{zp} - \mathbf{zp_c}}) , \, \mathbf{zp_c} + \mathbf{x_2} < \mathbf{r} < \mathbf{zp} \text{ (region III, interpolation)} \tag{20}$$

$$\Delta\varepsilon(\mathbf{r}) = \frac{\Delta K \cdot (1+\nu)}{\kappa E \sqrt{2\pi (\mathbf{r} - \mathbf{zp}/2)}} , \, \mathbf{r} \geq \mathbf{zp} \text{ (region IV, shifted Irwin)} \tag{21}$$

where $\kappa = 1$ for plane stress and $\kappa = 1/(1 - 2\nu)$ for plane strain, and

$$\mathbf{zp} = \frac{1}{\pi\kappa^2} \cdot \left(\frac{K_{\mathbf{max}}}{S_{\mathbf{Yc}}}\right)^2 \text{ and } \mathbf{zp_c} = \frac{1}{4\pi\kappa^2 \cdot (1+\mathbf{h_c})} \cdot \left(\frac{\Delta K}{S_{\mathbf{Yc}}}\right)^2 \tag{22}$$

9

Fig.3: Proposed strain range distribution, divided in 4 regions to consider both the elastic and the plastic contributions to the damage ahead of the crack tip.

Both constant (CA) and variable amplitude (VA) FCG can then be calculated using equations (18-22), which consider all the damage ahead of the crack tip and provide a more realistic model of the FCG process. But (2), (5) and (13) must be modified to include elastic parameters σ_c and **b**, and to account for the mean load σ_m effects on the VE life using Morrow elastic, Morrow elastic-plastic or Smith-Topper-Watson equations. But the life **N** in these equations cannot be explicitly written as a function of the VE strain range and mean load and thus must be calculated numerically, a programming task that, despite introducing no major conceptual difficulty, is far from trivial.

Variable Amplitude Loading

The **da/dN×ΔK** curve predicted for CA loads could be used with a FCG load interaction model for treat VA problems [17]. But the idea here is to *directly* quantify the fatigue damage induced by the VA load considering the crack growth as caused by the sequential fracture of *variable* size VE ahead of the crack tip. Since the Linear strain concentration rule generated better predictions above, it is the only one used here, and as load interaction effects can have a significant importance in FCG, they are modeled by using Morrow elastic equation to describe the VE fatigue life:

$$N(r+X) = \frac{1}{2}\left(\frac{\Delta\varepsilon_p(r+X)}{2\varepsilon_c}\left(1-\frac{\sigma_m}{\sigma_c}\right)^{-c/b}\right)^{1/c} \tag{23}$$

To account for mean load effects, a modified stress intensity range can be easily implemented for $\mathbf{R} > \mathbf{0}$ to filter the loading cycles that cause no damage by using:

$$\Delta K_{eff} = K_{max} - K_{PR} = \frac{\Delta K}{1-R} - K_{PR} \tag{24}$$

where $\mathbf{K_{PR}}$ is a propagation threshold that depends on the considered retardation mechanism, such as $\mathbf{K_{op}}$ or $\mathbf{K_{max}}^*$ from the Unified Approach [7]. The damage function for each cycle is then:

$$d_i(r+X_i) = \frac{n_i}{N_i(r+X_i)} \tag{25}$$

If the material ahead of the crack is supposed virgin, then its increment $\mathbf{\delta a_1}$ caused by the first load event is the value $\mathbf{r = r_1}$ that makes Equation (30) equal to one, therefore:

$$d_1(r_1+X_1) = 1 \quad \Rightarrow \quad \delta a_1 = r_1 \tag{26}$$

In all subsequent events, the crack increments account for the damage accumulated by the previous loading, in the same way it was done for the constant loading case. But as the coordinate system moves with the crack, a coordinate transformation of the damage functions is necessary:

$$D_i = \sum_{j=1}^{i} d_j\left(r + \sum_{p=j}^{i-1} \delta a_p\right) \tag{27}$$

Since the distance $\mathbf{r = r_i}$ where the accumulated damage equals one in the $\mathbf{i}$-th event is a variable that depends on $\mathbf{\Delta K_i}$ (or $\mathbf{\Delta K_{eff_i}}$) and on the previous loading history, VE of different widths may be broken at the crack tip by this model. This idea is illustrated in Fig. 4.

Experimental Results

FCG tests under VA loading were performed on API-5L-X52 steel $\mathbf{50 \times 10mm}$ C(T) specimens, pre-cracked under CA at $\mathbf{\Delta K = 20MPa\sqrt{m}}$ until reaching crack sizes $\mathbf{a \cong 12.6mm}$. These cracks were measured within $\mathbf{20\mu m}$ accuracy by optical methods and by a strain gage bonded at the back face of the specimens. The basic monotonic and cyclic properties, measured in computer-controlled servo-hydraulic machines using standard testing procedures, are $\mathbf{E = 200 \cdot 10^3}$, $\mathbf{S_U = 527}$, $\mathbf{S_Y = 430}$, $\mathbf{S_{Yc} = 370}$, $\mathbf{H_c = 840}$, and $\mathbf{\sigma_c = 720}$ (all in MPa), $\mathbf{h_c = 0.132}$, $\mathbf{\varepsilon_c = 0.31}$, $\mathbf{b = -0.076}$ and $\mathbf{c = -0.53}$.
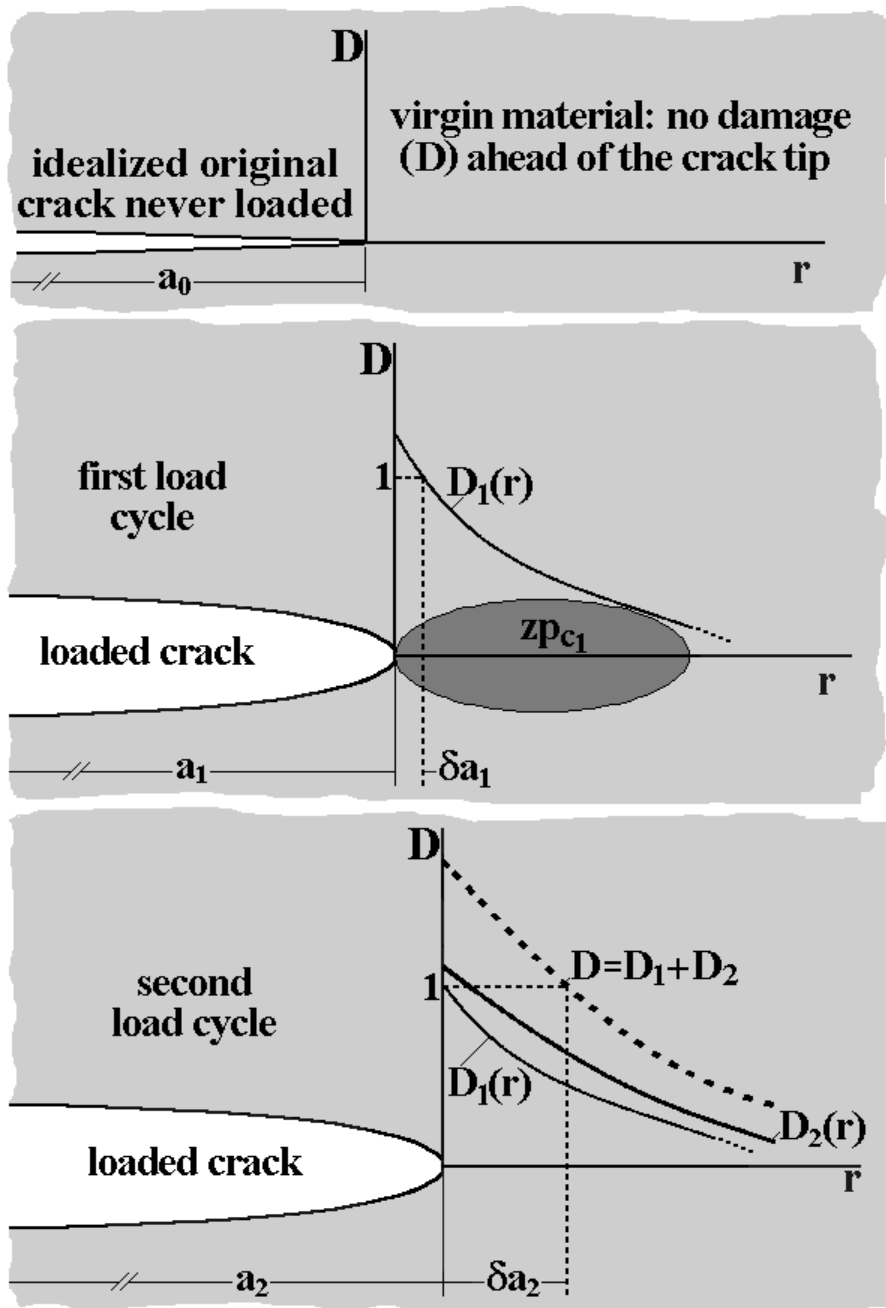
Fig.4: Schematics of the critical damage calculations, which under variable amplitude loading recognize variable crack increments by forcing the crack to grow over the region where **D = 1**.

About 50 εN specimens were tested under deformation ratios varying from **R = −1** to **R = 0.8** (at least 2 specimens were tested at each strain range) to measure the mean load effect on the (fatigue crack initiation) εN curve, see Fig. 5. Morrow's strain-life equation (25), which includes the mean stress effect only in Coffin-Manson's elastic term, best fit this experimental data. The basic **da/dN** curve, measured using the same equipment, was well fitted by a modified Elber-type equation **da/dN(R = 0.1) = 2·10^{-10}(ΔK − 8)$^{2.4}$** (**da/dN** in **m/cycle** and **ΔK** in **MPa√m**), using the crack propagation threshold **ΔK$_{th}$(R = 0.1) = 8MPa√m** to replace **K$_{op}$**.
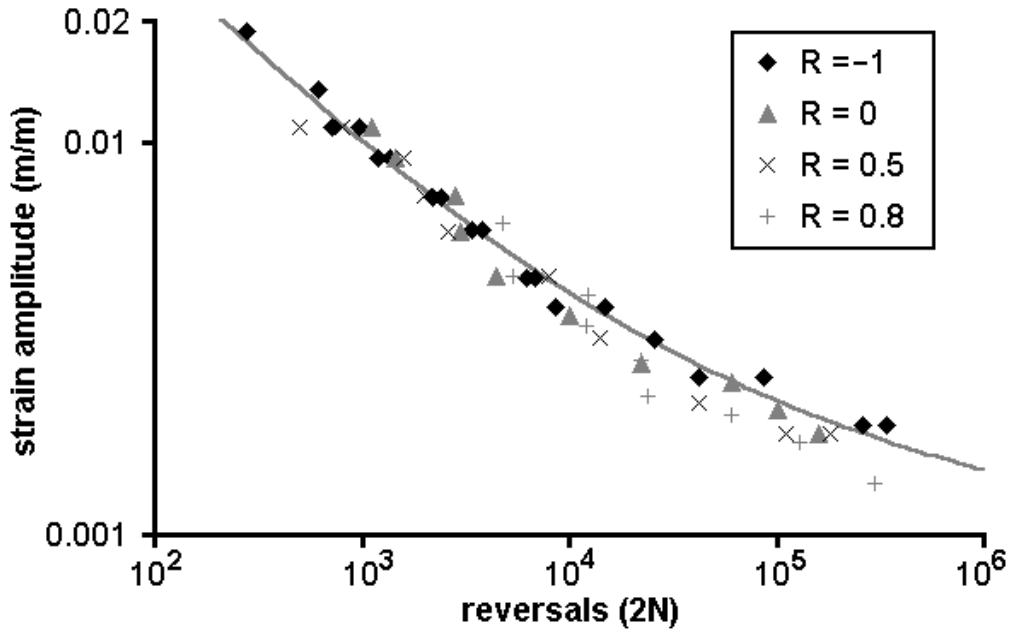
Fig.5: API 5L X52 steel strain-life data, and Morrow elastic model that best fitted this data.

FCG tests were then conducted under several VA histories. The history shown in Fig. 6 had 50,000 blocks containing 100 reversals each. Note the high mean stress levels, which were chosen to avoid crack closure effects (the crack was always opened during the loading). The load history was counted by the sequential rain-flow method, using the **ViDa** software [15]. The damage calculation was made using a specially developed code following all the procedures discussed above.

The crack growth predictions based solely on ε**N** parameters are again quite reasonable, see Fig. 7. The prediction assuming no damage outside the cyclic plastic zone **zp_c** underestimated the crack growth. However, when the small (but significant) damage in the material between the cyclic and monotonic plastic zone borders is also included in the calculations, an even better agreement is obtained. Note also that crack growth is slightly underestimated after $1.8 \cdot 10^6$ cycles, probably because these calculations neglected the (small) elastic damage and its mean stress effects.

A similar VA fatigue crack propagation test was conducted on a specimen of AISI 1020 steel, with measured properties **E = 205GPa, S_U = 491, S_Y = 285, S_{Yc} = 270, H_c = 941** and **σ_c = 815MPa, h_c = 0.18, ε_c = 0.25, b = −0.114**, and **c = −0.54**. The best FCG curve fitted to this material was slight more complex [17], **da/dN = $5 \cdot 10^{-10} \cdot (\Delta K - \Delta K_{th})^2 \cdot \{K_c/[K_c - \Delta K/(1 - R)]\}$**, where **$\Delta K_{th}$ = 11.6** and **K_c = 277** (**ΔK, ΔK_{th}** and **K_c** in **MPa√m** and **da/dN** in **m/cycle**).

The VA load history is this case was a series of blocks containing 101 peaks and valleys, as shown in Fig. 8. Fig. 9 compares the prediction with the measured data. This prediction was again quite reasonable. Therefore, one can claim that these tests indicate that the ideas behind the proposed critical damage model make sense and deserve to be better explored.
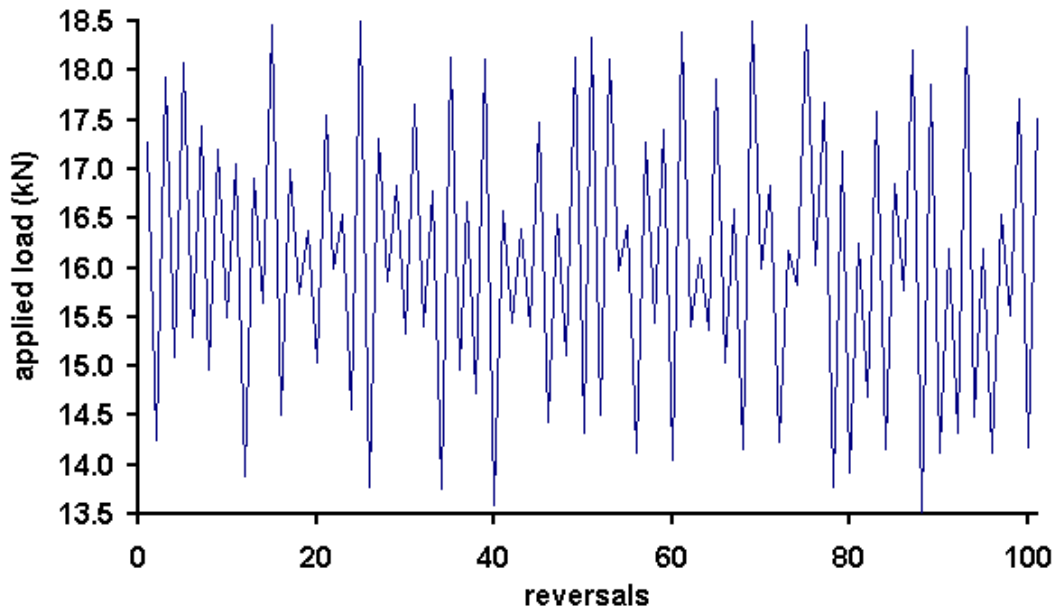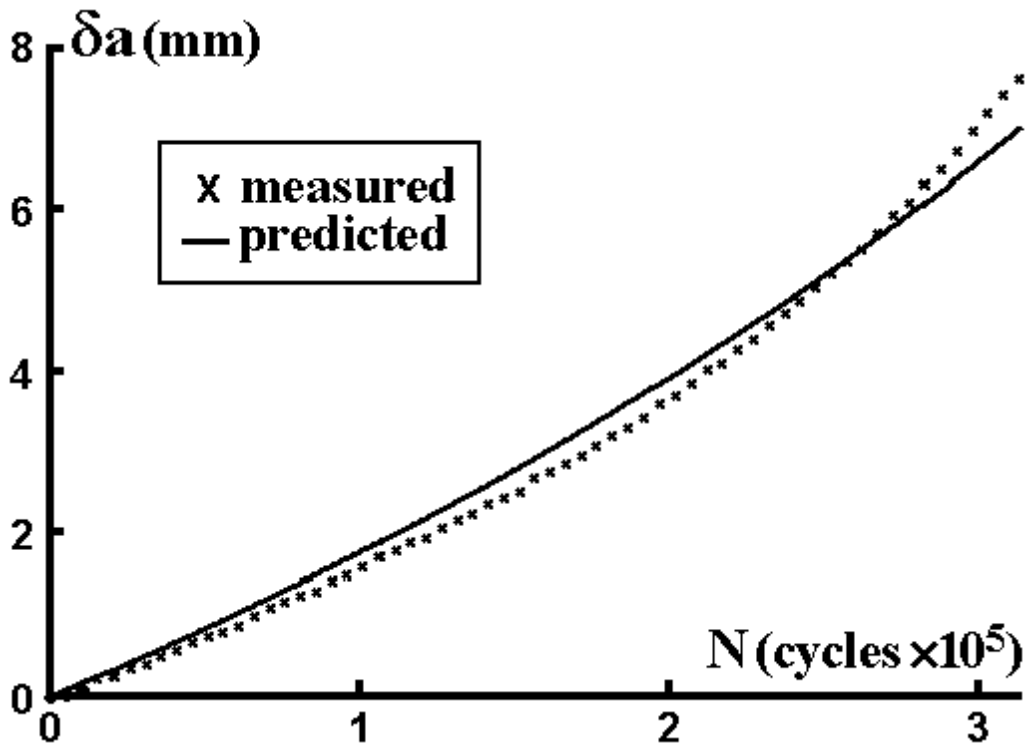

Fig.6: Variable amplitude load block applied to the API-5L-X52 steel. Note the high mean R-ratio.
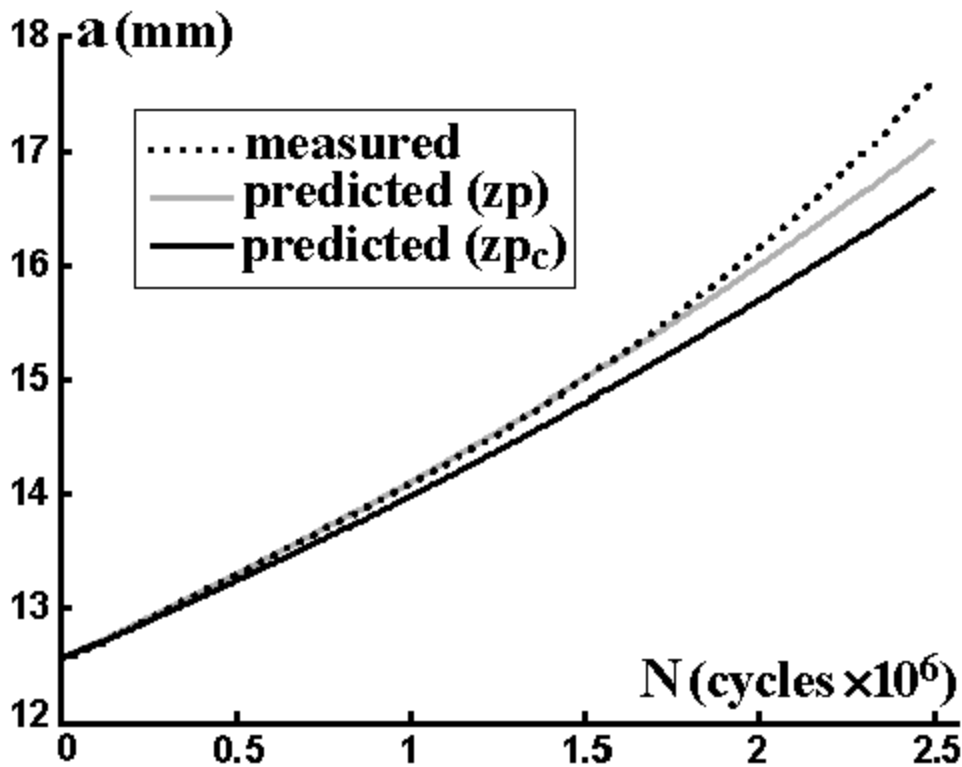
Fig.7: Comparison between the crack growth measurements and the εN-based predictions for the variable amplitude load presented in Fig. 6 (API-5L-X52 steel).
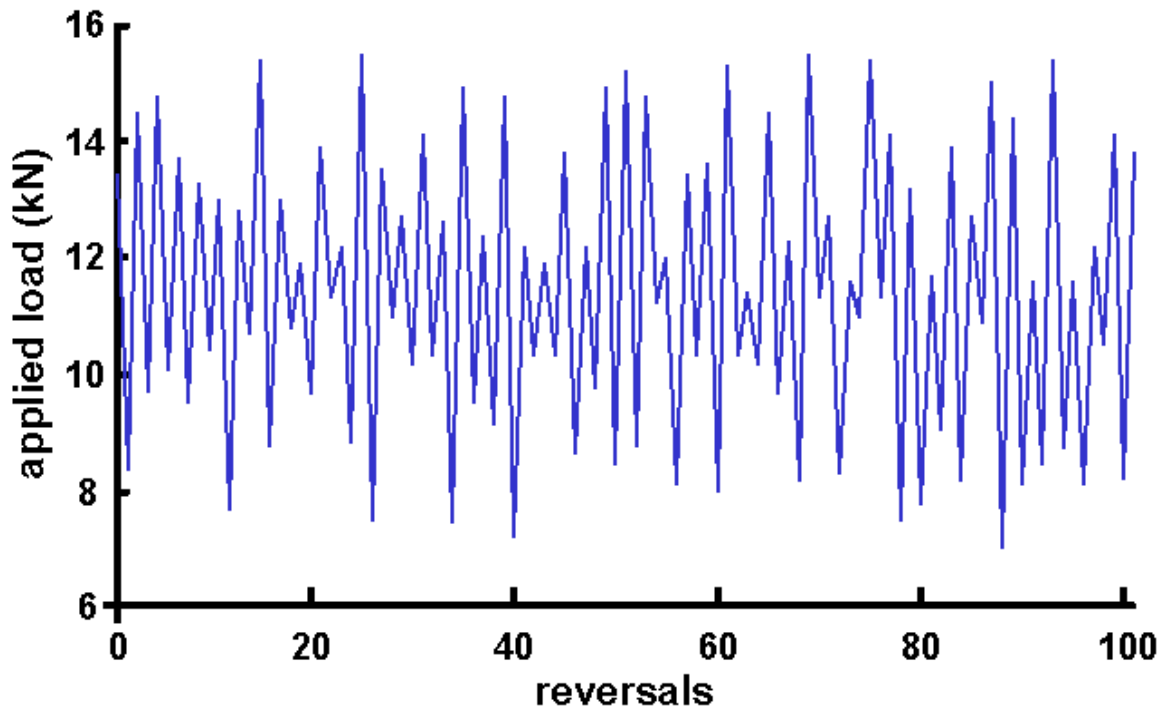
Fig.8: VA load block applied to the SAE 1020 steel C(T). Again a high mean R-ratio was used in this test, to avoid the interference of possible significant closure effects which could mask the model performance.

Fig.9: Comparison between the crack growth measurements and the εN-based predictions for the variable amplitude load presented in Figure 46 (SAE 1020 steel).

Conclusions

Several mechanisms can cause load sequence effects on fatigue crack growth, and they may act *before*, *at* or *after* the crack tip. Plasticity-induced crack closure is the most popular of them, but it cannot explain sequence effects in various important problems. A damage accumulation model ahead of the crack tip based on εN cyclic properties, which can explain those effects in the absence of closure, was proposed for predicting fatigue crack propagation under variable amplitude loading. The model treats the crack as a sharp notch with a small but finite radius to avoid singularity problems, and calculates damage accumulation explicitly at each load cycle. Experimental results show a good agreement between measured crack growth both under constant and variable amplitude loading and the predictions based purely on εN data.

References

[1] Majumdar,S; Morrow,J. Correlation Between Fatigue Crack Propagation and Low Cycle Fatigue Properties, ASTM STP 559, 159-182, 1974.
[2] Durán,JAR; Castro,JTP; Payão Filho,JC. Fatigue Crack Propagation Prediction by Cyclic Plasticity Damage Accumulation Models, FFEMS 26, 137-150, 2003.
[3] Suresh,S. *Fatigue of Materials*, 2nd ed., Cambridge, 1998.
[4] Skorupa,M. Load Interaction Effects During Fatigue Crack Growth under Variable Amplitude Loading - a Literature Review - Part I: Empirical Trends, FFEMS 21, 987-1106, 1998.
[5] Skorupa,M. Load Interaction... Part II: Qualitative Interpretation, FFEMS 22, 905-926, 1999.
[6] Castro,JTP; Meggiolaro,MA; Miranda,ACO. Singular and Non-Singular Approaches for Predicting Fatigue Crack Growth Behavior, IJ Fatigue 27, 1366-1388, 2005.
[7] Vasudevan,AK; Sadananda,K; Holtz,RL. Analysis of Vacuum Fatigue Crack Growth Results and its Implications, IJ Fatigue 27, 1519-1529, 2005.
[8] Meggiolaro,MA; Castro,JTP. On the Dominant Role of Crack Closure on Fatigue Crack Growth Modeling, IJ Fatigue 25, 843-854, 2003.
[9] Schwalbe,KH. Comparison of Several Fatigue Crack Propagation Laws with Experimental Results, Eng. Fracture Mechanics 6, 325-341, 1974.
[10] Glinka,G. A Notch Stress-Strain Analysis Approach to Fatigue Crack Growth, Eng. Fracture Mechanics 21, 245-261, 1985.
[11] Creager,M: Paris,PC. Elastic Field Equations for Blunt Cracks with Reference to Stress Corrosion Cracking, IJ Fracture Mechanics 3, 247-252, 1967.
[12] Neuber,H. Theory of Stress Concentration for Shear-Strained Prismatical Bodies with an Arbitrary Non-Linear Stress-Strain Law, J. Applied Mechanics 28, 544-551, 1961.
[13] Molsky,K; Glinka,G. A Method of Elastic-Plastic and Strain Calculation at a Notch Root, Materials Science and Engineering 50, 93-100, 1981.
[14] Stephens,R; Fatemi,A; Stephens,RR; Fuchs,HO. *Metal Fatigue in Engineering*, Interscience, 2000.
[15] www.tecgraf.puc-rio.br/vida
[16] Parton,VZ; Morozov,EM. *Elastic-Plastic Fracture Mechanics*, Mir Publishers, 1978.
[17] Castro,JTP; Meggiolaro,MA. *Fadiga sob Cargas Reais de Serviço*, LTC (in press).